

Received March 25, 2019, accepted April 21, 2019, date of publication May 1, 2019, date of current version May 15, 2019.

Digital Object Identifier 10.1109/ACCESS.2019.2914232

Radar Moving Target Detection in Clutter Background via Adaptive Dual-Threshold Sparse Fourier Transform

XIAOHAN YU^{ID}, XIAOLONG CHEN^{ID}, (Member, IEEE), YONG HUANG, LIN ZHANG,
JIAN GUAN, (Member, IEEE), AND YOU HE

Radar Target Detection Research Group, Naval Aviation University, Yantai 264001, China

Corresponding author: Xiaolong Chen (cxlx11209@163.com)

This work was supported in part by the National Natural Science Foundation of China under Grant 61871391, Grant U1633122, Grant 61871392, and Grant 61531020, in part by the Project of Shandong Province Higher Educational Science and Technology Program under Grant J17KB139, and in part by the Special Funds of Young Talents Program of CAST.

ABSTRACT In this paper, an adaptive dual-threshold sparse Fourier transform (ADT-SFT) algorithm is proposed, which enables the application of the SFT and robust SFT (RSFT) to the moving target detection in clutter background. Two levels of detection are introduced in this algorithm. First, a scalar constant false alarm rate (CFAR) detection is employed in each frequency channel formed by subsampled fast Fourier transform (FFT) to suppress the influence of strong clutter points on the sparsity and frequencies estimation. Second, the subspace detector constructed by suspected target Doppler frequencies is adopted to complete the target detection. The simulation analysis and results of the measured sea clutter data show that the ADT-SFT algorithm is more suitable for the clutter background and can obtain better detection performance than SFT and RSFT. In addition, compared with the conventional subspace detection (SD) algorithm, which needs to search all the Doppler frequencies one-by-one to establish the detector, the ADT-SFT algorithm only needs to search a small number of suspected target Doppler frequencies, and therefore, the computational complexity can be greatly reduced.

INDEX TERMS Moving target detection, sparse Fourier transform (SFT), adaptive dual-threshold sparse Fourier transform (ADT-SFT), constant false alarm rate (CFAR) detection, subspace detection (SD).

I. INTRODUCTION

Fast and reliable detection of moving target in clutter background has always been a hot and difficult problem in radar signal processing. Influenced by the complex clutter background and complex motions, the target returns often exhibit low-observable characteristics, which would increase the difficulty of radar detection [1], [2]. With the development of new radar systems, e.g. phased array radar, staring observation radar, and multi-input and multi-output (MIMO) radar, the observation time of target can be greatly prolonged, which is beneficial to increase the integration gain and improve the detection performance of weak target in clutter background. However, this staring observation mode will cause a large number of time serials and Doppler channels, which makes the traditional moving target detection (MTD) method

very time-consuming. Moreover, the increment of sampling frequency would further result in big data, and thus higher efficiency and real-time processing ability are required for real applications [3]. Therefore, it is of great significance to investigate signal processing and detection methods which are supposed to be sufficient, reliable, suitable for large amount of data and clutter background.

In recent years, the theory of sparse signal processing technology provides a new solution for radar detection [4]–[11]. Since the moving target's returns would exhibit sparse characteristics in a certain domain, the moving target detection problem can be converted into the sparse decomposition and detection problem in the sparse domain. And high resolution representation of the signal can be achieved in the sparse domain using a small number of observation samples via optimization calculations. At present, the sparse representation-based moving target detection methods are mainly divided

The associate editor coordinating the review of this manuscript and approving it for publication was Chengpeng Hao.

into three categories. The first solution is from the perspective of sparse decomposition of mixed signals and then it would result in different features in sparse domain, which are useful for target detection. For example, a micro-motion target detection and feature extraction method based on morphological component analysis (MCA) is proposed in [6]. Different dictionaries are designed and used for sparse representation to distinguish clutter and moving target. This kind of methods require a precise signal model for target, and selection of the dictionary for sparse representation is the key point accordingly. The second and third solutions all combine the advantages of time-frequency distribution (TFD) and sparse representation. The differences are that the former one is from the perspective of sparse optimization to construct the sparse time-frequency transform domain and the latter one employs the idea of subsampled sparse Fourier transform (SFT). In this way, high-resolution, low-complexity time-frequency representation of the time-varying signal in the time and sparse domain can be achieved. The second solution has good adaptive performance for different kinds of signals, but the sparse optimization is very complicated and would increase the computation cost. For the third solution, due to the combination of fast FT (FFT) and sparse representation, it is good at analysis of long-time serials. The most typical one is the SFT [11] proposed by Hassanieh et al. from Massachusetts Institute of Technology (MIT). The SFT was awarded as one of the top ten disruptive technologies in 2012 by the MIT Technical Review. The core idea of the algorithm is to convert the N -point long sequence into a B -point short sequence through random spectrum permutation, flat-window filtering and time domain aliasing (corresponding to the frequency domain subsampling), then the FFT is done on the short sequence. Therefore, SFT is more efficient than the classical FFT. For an N -points size signal with a sparse spectrum, SFT can reduce the computational complexity of FFT to $O(K \log_2 N)$, where K is the sparsity of signal, i.e. the number of large coefficients in frequency domain [12]–[14]. And a bigger K means more sparsity of the signal. The SFT method has been effectively used in spectrum sensing, image detection, medical imaging, etc. If it can be applied to radar target detection, it is expected to improve the detection efficiency [15]–[17].

However, SFT has several defects considering the requirements for real applications. On the one hand, most SFT methods need to preset the sparsity of the signal, but the sparsity is often unknown or subject to change. On the other hand, after subsampling in frequency domain, SFT estimates the large frequency coefficients only utilizing the information of sparsity and occurrence probability of frequencies in the loop. It is difficult to guarantee the reliability of reconstructed signal in the case of low signal-to-clutter and noise ratio (SCNR) condition. Therefore, the SFT-based detection method cannot meet the requirements of radar moving target detection in complex environments. Many scholars at home and abroad have improved the SFT method from the perspectives of sparsity estimation, Fourier coefficients estimation correction, and closed-form expression derivation [18]–[20].

Among them, the robust SFT (RSFT) algorithm proposed in [20] is a typical one and it includes two stages of detection using the Neyman-Pearson criterion. RSFT does not require knowledge of the exact sparsity of the signal and is robust to noise. RSFT uses the previously calculated noise threshold to make decision and thus is more suitable for the detection in the white noise background. However, radar target detection usually faces clutter background and the clutter is often much stronger than noise with the frequency spectrum nonuniformly distributed, such as sea clutter. Moreover, the strong clutter points in frequency domain will also cause bigger sparsity, which would greatly degrade the reconstruction performance. In addition, both SFT and RSFT algorithms declare a target or not while reconstructing the target's Doppler spectrum. This decision is made on the condition that flat-window filtering reduces the SCNR. Therefore, SFT and RSFT are ineffective for moving target detection in clutter background. From the above analysis, there are three problems to be solved: 1) The conventional FFT-based subspace detection (SD) method requires one-by-one search of all Doppler channels, which will result in heavy computational burden. 2) SFT needs to know the exact sparsity of target, which is difficult to estimate in practice. 3) The signal reconstruction of SFT and RSFT is greatly influenced by SCNR, and lower SCNR results in poor detection performance.

To solve these problems, a novel moving target detection algorithm is proposed in this paper named as adaptive dual-threshold SFT (ADT-SFT). Firstly, the Doppler frequencies of suspected target are obtained based on the first adaptive threshold. Then, a subspace detector, which is the second judgment, is constructed for the final target detection. The advantage of ADT-SFT compared with the conventional SD method is the reduction of complexity, because it only performs SD on the suspected target frequencies rather than all the frequencies of the spectrum. The thresholds of the two detection stages are adaptive to the clutter background. Simulations and real experiments all indicate that, compared with SFT and RSFT, the ADT-SFT is not only suitable for moving target detection in complex clutter background, but also can meet the actual requirements for large amount of computations.

Notation: The parameters commonly used in this paper are listed as follows. N is the number of pulses. B is the number of buckets, namely the length of short sequence. M is the number of location loops. f_d denotes the center frequency of target, f_s denotes the pulse repetition frequency (PRF). η_1 and η_2 are the first and the second threshold, respectively. w denotes the Occurrence Value. In SFT algorithm, K denotes the preset sparsity, while in ADT-SFT algorithm, K is the estimated sparsity obtained by the first detection threshold. H is the number of suspected target frequencies obtained by reconstruction.

The remaining of the paper is organized as follows. The echo model corresponding to the detection problem is established in section II. In section III, the basic principles of SFT and RSFT algorithms are introduced, and the disadvantages

in clutter background are illustrated by simulation results. In section IV, the proposed ADT-SFT algorithm is explained in detail and the detection procedure of ADT-SFT based moving target detection method is described in section V. In section VI, the detection performance and computational complexity of the proposed algorithm are analyzed by simulation experiments and measured radar data in sea clutter background. The last section concludes the paper and presents its future research directions.

II. ECHO MODEL OF TARGET

Assume that radar transmits a coherent pulse train with single carrier frequency, and the target moves uniformly during the observation time. After mixing and matched filtering, the radar returns can be modeled as

$$s(n) = A_s \exp [j(2\pi f_d n T + \varphi_s)], \quad n = 0, 1, \dots, N-1 \quad (1)$$

where A_s is the amplitude, $f_d = 2v/\lambda$, v denotes the speed of target, λ is the wavelength, T is the pulse repetition period (PRI), and φ_s is the phase. And we assume that the target echo amplitude is not undulated among pulses.

Under the SFT framework, if the observation time is too long, which results the change of target Doppler. The target echo cannot be modeled as the single-frequency signal shown in (1). Instead, it can be expressed as the subspace target consisting of I adjacent Doppler frequencies, as shown in (2). The range migration caused by long-time integration is not our focus and will not be discussed in this paper.

$$s(n) = \sum_{i=1}^I A_{s,i} \exp [j(2\pi f_{d,i} n T + \varphi_{s,i})], \quad n = 0, 1, \dots, N-1 \quad (2)$$

In case of clutter background, during the observation time NT , the radar echo model can be expressed as

$$x(n) = \begin{cases} s(n) + c(n), & H_1 \\ c(n), & H_0 \end{cases} \quad (3)$$

where $c(n)$ denotes clutter, $n = 0, 1, \dots, N-1$.

III. SFT ALGORITHM

A. THEORETICAL FRAMEWORK OF SFT

At a high level, SFT algorithm works by binning the Fourier coefficients into a small number of buckets [11]. So the N -point long sequence is converted into B -point short sequence, and FFT is done on the short sequence, where N/B is the capacity of the bucket. Since the signal is sparse in the frequency domain, each bucket is likely to have only one large coefficient. Then, the buckets which contain large coefficients are selected. Finally, the reconstruction method corresponding to the binning rules is designed to restore the complete signal spectrum. Fig. 1 shows the basic theoretical framework of SFT algorithm.

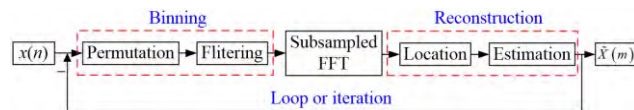


FIGURE 1. Basic theoretical framework of SFT.

1) BINNING

To make separation of the nearby coefficients in frequency domain, a permutation is performed on the time domain signal $x(n)$. Define a permutation function P_ξ , and the time domain signal after permutation can be expressed as

$$P_\xi(n) = x [(\xi n) \bmod N], \quad n \in [1, N] \quad (4)$$

where $\xi \in [1, N]$ is a random odd number that is invertible mod N , and mod represents the modulo operation.

Define a flat-window $g(n)$, its frequency domain expression $G(m)$ satisfies

$$G(m) \in \begin{cases} [1 - \delta, 1 + \delta], & m \in [-\varepsilon'N, \varepsilon'N] \\ [0, \delta], & m \notin [-\varepsilon N, \varepsilon N] \end{cases} \quad (5)$$

where ε' and ε denote the passband truncation factor and the stopband truncation factor respectively, δ is the extent of ripple oscillation. Define a signal $y(n) = g(n) \cdot P_\xi(n)$, $n \in [1, N]$, and the support of $y(n)$ satisfies $\text{supp}(y) \subseteq \text{supp}(g) = [-\omega/2, \omega/2]$, ω is the length of window.

2) SUBSAMPLED FFT

Suppose B is an integer that exactly divide N , the signal after subsampled FFT can be expressed as

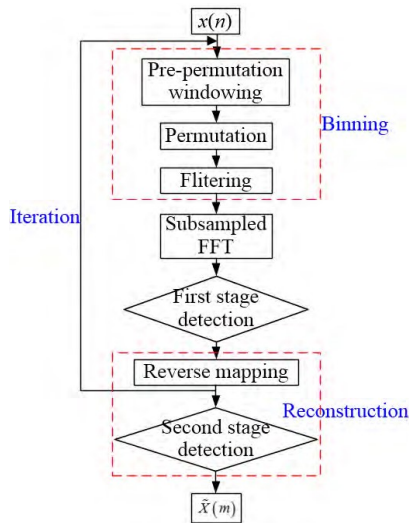
$$Z(m) = \text{FFT} \left\{ \sum_{j=0}^{\lfloor \omega/B \rfloor - 1} y(n + jB), n \in (1, B) \right\} \quad (6)$$

where $\lfloor \cdot \rfloor$ denotes the down-rounding operation.

3) RECONSTRUCTION

The reconstruction consists of two loops, namely location loop and estimation loop, where location loop finds the indexes of the K largest Fourier coefficients in the original signal spectrum, and estimation loop calculates the corresponding coefficients. In this paper, the location is emphasized more than estimation, since the locations of frequencies are directly related to target parameters in radar moving target detection.

Define a mapping function $h_\xi(m) = \lfloor \xi \cdot m \cdot B/N \rfloor$, and a set J , where J contains the K coordinates of the maximum magnitudes in $Z(m)$. Output the preimage by reverse mapping, i.e., $U = \{m \in [1, N] | h_\xi(m) \in J\}$, the size of U is $K \cdot N/B$. However, the set U contains not only the locations of large frequency coefficients, but also many other ambiguous locations caused by aliasing. To remove the ambiguous locations, multiple location loops with random permutations are performed. More details about the SFT theory can be found in [11].

**FIGURE 2.** RSFT schematic diagram.

B. PRINCIPLE OF RSFT

The RSFT algorithm is proposed on the basis of SFT theoretical framework. Fig. 2 shows the schematic diagram of RSFT, and compared with SFT, it introduced two levels of detection. The first level detection is based on the symmetric Gaussian distribution assumption and is performed on the subsampled FFT results $Z(m)$ (as shown in (6)), and can be expressed as [20]

$$|Z(m)| \begin{cases} > \frac{H_1 \gamma - \log(\sigma_1^2/\sigma_2^2)}{1/\sigma_1^2 - 1/\sigma_2^2} \\ < H_0 \end{cases} \quad (7)$$

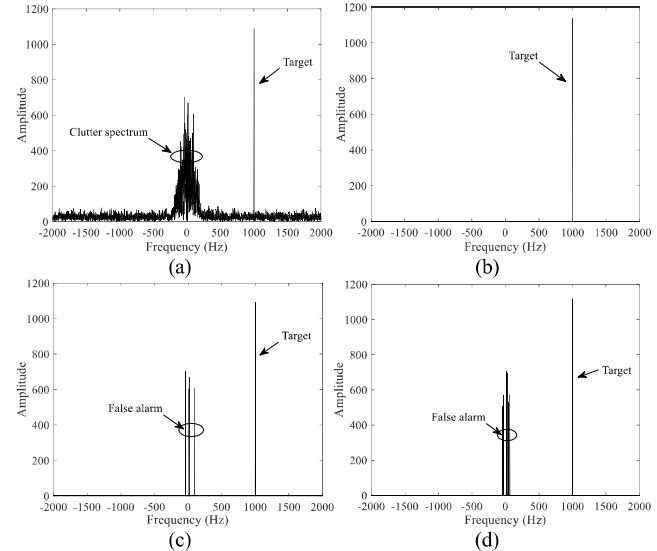
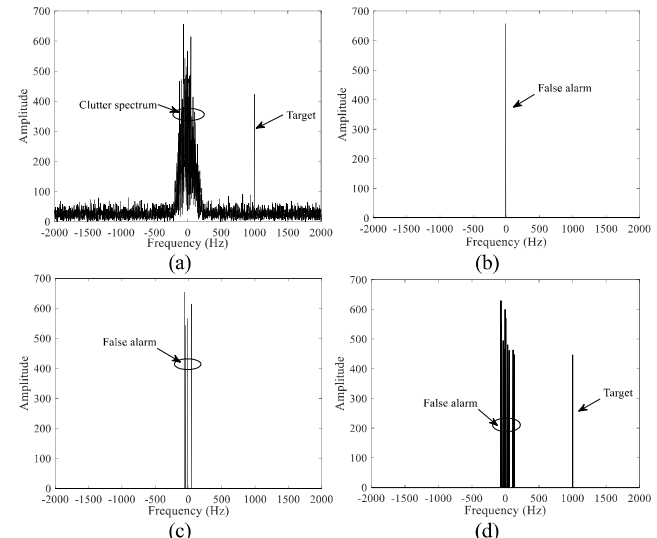
where σ_1^2 denotes the noise variance of the Fourier coefficients in the bucket without significant frequency, σ_2^2 denotes the noise variance of the Fourier coefficients in the bucket with significant frequency, γ is a threshold. The second stage detection suppose that the variable after reverse mapping and accumulation is the summation of Bernoulli variables with different success rates. This detection is also a judgment related to the noise background. Compared with SFT, RSFT does not require knowledge of the exact sparsity of the signal and is robust to noise.

C. DEFECTS OF SFT AND RSFT

Based on the above introduction, the SFT and RSFT have two following insufficient points when dealing with moving target detection in clutter background.

1) The SFT algorithm directly takes the frequencies corresponding to the K largest coefficients in the subsampled spectrum as the estimation result of target frequencies, where K is either known in advance or roughly estimated. It is easy to be disturbed by strong clutter frequencies. Although RSFT makes some improvements by setting two thresholds, it is only suitable for the noise background.

2) Both SFT and RSFT algorithms detect the target while performing the reconstruction. In fact, this detection is made

**FIGURE 3.** Results of SFT and RSFT ($f_d = 1000$ Hz, SCNR= -12 dB). (a) FFT spectrum. (b) SFT ($K = 1$). (c) SFT ($K = 4$). (d) RSFT.**FIGURE 4.** Results of SFT and RSFT ($f_d = 1000$ Hz, SCNR= -20 dB). (a) FFT spectrum. (b) SFT ($K = 1$). (c) SFT ($K = 4$). (d) RSFT.

on the basis of frequencies obtained in the subsampled spectrum and the frequencies occurrence probabilities during the reconstruction. However, the flat-window filtering implemented before subsampled FFT essentially would reduce the SCNR of the target frequencies, so this detection is not conducive to the problem of target detection in the clutter background.

The above two points are illustrated by the following simulations. Suppose there is a target moving towards to radar. The spectral center of the clutter is 0 Hz, 3 dB spectral width is about 200 Hz, clutter-to-noise ratio is 15 dB. $f_s = 5000$ Hz, $T = 0.0002$ s, $N = 4096$, $B = 256$, $M = 100$. Fig. 3 and Fig. 4 show the results of SFT and RSFT under different SCNR when target spectrum does not fall into the clutter

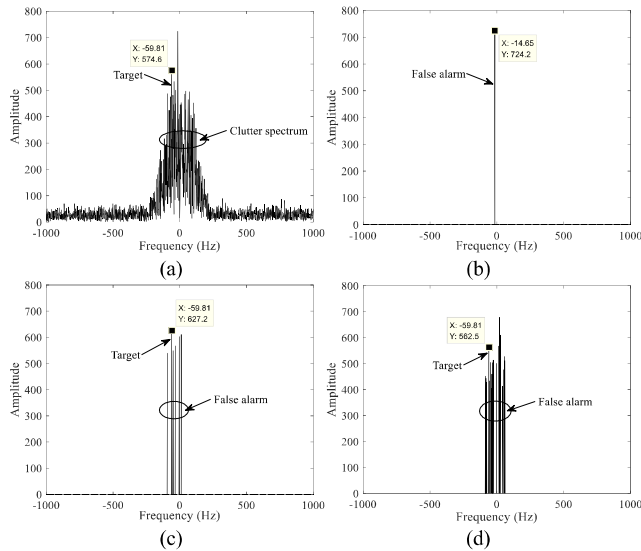


FIGURE 5. Results of SFT and RSFT ($f_d = -59.8$ Hz, SCNR = -20 dB). (a) FFT spectrum. (b) SFT ($K = 1$). (c) SFT ($K = 6$). (d) RSFT.

spectrum ($\lambda = 0.03$ m, $v = 15$ m/s, $f_d = 1000$ Hz). Fig. 3 corresponds to the case when SCNR is higher (SCNR = -12 dB), that is, the amplitude at the target frequency is larger than the amplitude of the clutter frequencies in the spectrum. Fig. 3 (a) is the FFT spectrum of the echo data obtained without considering the complexity. Fig. 3 (b) and Fig. 3 (c) show the SFT results of $K = 1$ and $K > 1$, respectively, and Fig. 3 (d) gives the result of RSFT. It can be seen that when $K = 1$ (just coincides with the target number), the SFT algorithm can effectively detect the target, while when K is set to be greater than 1, the false alarms are generated in the SFT result. In contrast, RSFT produces more false alarms because the noise threshold given by the algorithm is significantly lower than the required threshold in clutter background. Fig. 4 corresponds to the case when SCNR is lower (SCNR = -20 dB). In this case, both SFT and RSFT algorithm result in more false alarms and wrong target location as well.

Fig. 5 shows the results of SFT and RSFT when the target spectrum is totally covered by the clutter spectrum ($\lambda = 0.2$ m, $v = -5.98$ m/s, $f_d = -59.8$ Hz, SCNR = -20 dB). Compared with Fig. 3 and Fig. 4, it can be found that the processing results of the three figures are similar. Whether the target spectrum falls into the clutter spectrum or not, there are a number of false alarms in the results of SFT and RSFT,

especially in the lower SCNR case. The reason is that the flat-window filtering causes spectrum aliasing. Whatever the relative positions of the target and clutter are in the original FFT spectrum, they are uncertain in the spectrum which has been aliased.

The above simulation results show that the value of K has a great influence on the result of SFT algorithm, which would lower the robustness. Besides, the performances of SFT and RSFT will deteriorate greatly in clutter background especially in the case of low SCNR. In this condition, more false alarms will arise and the true target is missed. Therefore, it is necessary to investigate the algorithm suitable for clutter background.

IV. PRINCIPLE OF ADT-SFT

Compared with the SFT and RSFT algorithms, the ADT-SFT algorithm proposed two novel detection thresholds adaptive to the clutter background. On the one hand, it improves the estimation of target's Doppler spectrum after subsampling; on the other hand, it constructs the subspace detector for the detection of suspected target's Doppler after reconstruction. Fig. 6 shows the schematic diagram of ADT-SFT.

1) ESTIMATE THE SPARSITY AND FREQUENCIES OF TARGET USING THE FIRST THRESHOLD

The first threshold η_1 is employed in the subsampled spectrum $Z(m)$. Define a set J' , which contains the coordinates of frequencies whose amplitudes higher than η_1 in $Z(m)$, namely

$$J' = \{m \in [1, B] \mid Z(m) \geq \eta_1\} \quad (8)$$

then, output the preimage by reverse mapping, i.e.,

$$U' = \{m \in [1, N] \mid h_\xi(m) \in J'\} \quad (9)$$

The first threshold η_1 is determined by the scalar constant false alarm rate (CFAR) detection technique. For example, for the sea clutter background with low time stability and high spatial stability, the spatial domain CFAR detectors [21]–[23] such as the mean-level CFAR, the order-statistic CFAR, and the adaptive CFAR can be selected according to the background. For the spatial domain CFAR methods, more data from multiple reference rangebins are required to accommodate the changes of clutter background.

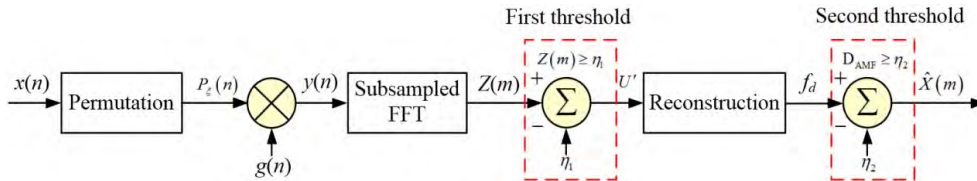


FIGURE 6. The proposed ADT-SFT schematic diagram.

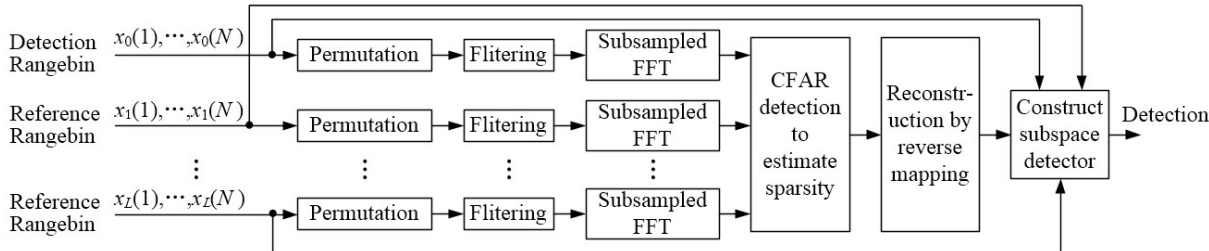


FIGURE 7. Flow chart of radar moving target detection based on ADT-SFT.

2) RECONSTRUCT THE SUSPECTED TARGET FREQUENCIES BY REVERSE MAPPING

Due to the characteristics of reverse mapping, M location loops are required in the reconstruction process [24]. If there is a target, the occurrence times of target's Doppler frequency should be higher in the location loops. Based on this assumption, we define the Occurrence Value w . And the frequencies whose occurrence times higher than w , are named as the suspected target Doppler frequencies. Since the reconstruction of target Doppler frequencies would be seriously affected by strong clutter in the frequency domain especially in low SCNR conditions, the false target Doppler frequencies may appear. And even worse, the true target Doppler frequencies cannot be reconstructed at all. Therefore, the Doppler frequencies f_d obtained by the reconstruction process are only the suspected ones, which need to be confirmed by the subsequent subspace detector.

3) PERFORM THE SUBSPACE DETECTOR TO COMPLETE THE FINAL DETECTION

The subspace detector is constructed by combining the original observation data in detection rangebin and reference rangebins, and the corresponding threshold is called the second threshold η_2 . The detection is performed on the suspected target Doppler frequencies to obtain the real target Doppler frequencies, and the corresponding spectrum $\hat{X}(m)$ is the final output of ADT-SFT.

Influenced by clutter background, target Doppler spread, multi-targets, η_1 , w , etc., multiple suspected target Doppler frequencies may be obtained by the reconstruction. At this time, if these Doppler frequencies are scattered or not close to each other, the *rank-1* subspace detector is designed to declare if there is a target. If these Doppler frequencies are concentrated or close to each other, i.e., the Doppler spread target, the *multi-ranks* subspace detector is employed to make the detection.

Rank-1 subspace detector: Assume that the suspected target Doppler frequency is f_{d0} , the target Doppler vector obtained from (1) can be expressed as

$$\vec{s}_0 = [1 e^{2\pi f_{d0} T} \dots e^{2\pi f_{d0} T(N-1)}]^T \quad (10)$$

and the observation vector obtained from (3) is

$$\vec{x} = [x_0 \ x_1 \ \dots \ x_{N-1}]^T \quad (11)$$

So the adaptive matched filter (AMF) subspace detector D_{AMF} [25] can be constructed as follows

$$D_{AMF} = \frac{\left| \vec{s}_0^H \mathbf{C}^{-1} \vec{x} \right|^2}{\vec{s}_0^H \mathbf{C}^{-1} \vec{s}_0} \begin{cases} H_1 & > \eta_2 \\ H_0 & \leq \eta_2 \end{cases} \quad (12)$$

where \mathbf{C} is the clutter covariance matrix estimated by reference rangebins, $(\cdot)^T$ and $(\cdot)^H$ denote the transpose and conjugate transpose of a matrix or a vector respectively.

Multi-ranks subspace detector: Suppose the suspected target Doppler frequencies are f_{d1}, \dots, f_{dI} , the target subspace matrix obtained from (2) can be expressed as

$$\mathbf{S} = [\vec{s}_1, \dots, \vec{s}_I] \quad (13)$$

where $\vec{s}_i = [1 e^{2\pi f_{di} T} \dots e^{2\pi f_{di} T(N-1)}]^T$, $i = 1, \dots, I$. So the AMF subspace detector can be represented as

$$D_{AMF} = \vec{x}^H \mathbf{C}^{-1} \mathbf{S} (\mathbf{S}^H \mathbf{C}^{-1} \mathbf{S})^{-1} \mathbf{S}^H \mathbf{C}^{-1} \vec{x}^H \begin{cases} H_1 & > \eta_2 \\ H_0 & \leq \eta_2 \end{cases} \quad (14)$$

V. MOVING TARGET DETECTION BASED ON ADT-SFT

The flow chart of radar moving target detection based on ADT-SFT is shown in Fig. 7, which specifically includes the following steps:

Step 1: Permutation: The spectrum permutation is performed with the original observation data $x_l(1), \dots, x_l(N)$, $0 \leq l \leq L$ according to (4), and $P_\xi^l(n)$, $n \in [1, N]$ refers to the permutation result.

Step 2: Filtering: Next the flat-window mentioned in (5) is adopted for filtering. The window filter $G(\varepsilon, \varepsilon', \delta, \omega)$ determines the mapping relations between the signal frequencies and each bucket. In order to ensure the efficiency and avoid the spectrum leakage, $G(\varepsilon, \varepsilon', \delta, \omega)$ should be concentrated both in time and frequency domains, the parameters setting are $\varepsilon = 1/B$, $\varepsilon' = 1/2B$, $\delta \approx 1/N$, $\omega = O(B \log N / \delta)$.

Step 3: Subsampled FFT: The operation is performed on the filtered signal according to (6). To balance the computational cost of the binning and estimation, the number of buckets can be taken as $B = O(\sqrt{N})$, and B is an integer which can exactly divide N [11].

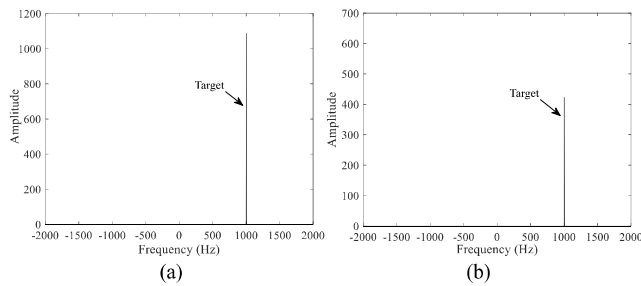


FIGURE 8. Results of ADT-SFT ($f_d = 1000$ Hz). (a) ADT-SFT (SCNR= -12 dB). (b) ADT-SFT (SCNR= -20 dB).

Step 4: First detection threshold: According to (8), the scalar CFAR detection namely the first threshold η_1 is used to estimate the signal sparsity and frequency points in the Doppler channels after frequency subsampling. At the same time, the original data can be processed by MTI or adaptive MTI (AMTI) before ADT-SFT, in order to further reduce the influence of the strong clutter points on the sparsity and frequency points estimation.

Step 5: Reconstruction: According to (9), output the original locations of interested frequencies by reverse mapping. And the frequencies whose occurrence numbers surpassing w in the location loops are considered to be the suspected target Doppler frequencies.

Step 6: Second detection threshold: Construct a subspace detector, and employ the second threshold η_2 to complete the detection. If the suspected target Doppler frequencies are scattered, construct the rank-1 subspace detector one by one according to (12) to make the decision. If the Doppler frequencies are multipoint adjacent, the multi-ranks subspace detector is constructed according to (14) to finish the detection.

VI. SIMULATION AND RESULTS ANALYSIS

In this section, the simulation and the real radar data are used to verify the performance of the proposed algorithm in clutter background. Firstly, the detection results of FFT, SFT, RSFT, and ADT-SFT are demonstrated for two scenarios, i.e., whether the target's spectrum falls into the clutter spectrum or not. Secondly, two typical radar datasets recorded by the X-band Council for Scientific and Industrial Research (CSIR) radar are employed to verify the detection performances for moving target in real sea clutter environment. Thirdly, the detection performance, i.e., SCNR versus detection probabilities, are compared and shown quantitatively by Monte Carlo simulations. At last, the relations between computational complexity and the detection performance are illustrated.

A. SIMULATION ANALYSIS

The same simulation data are used as section III C (Fig. 2 to Fig. 5). Fig. 8 and Fig. 9 show the results of ADT-SFT algorithm for the cases of $f_d = 1000$ Hz and $f_d = -59.8$ Hz, respectively. In Fig. 8, when the target spectrum does not

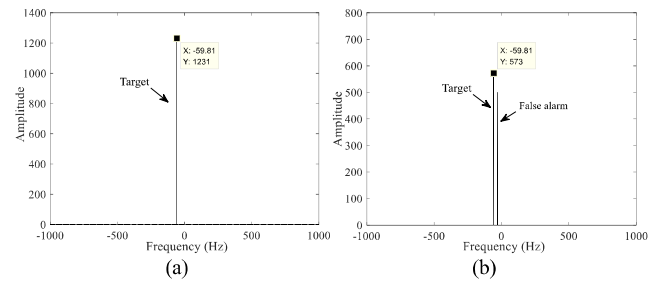


FIGURE 9. Results of ADT-SFT ($f_d = -59.8$ Hz). (a) ADT-SFT (SCNR= -12 dB). (b) ADT-SFT (SCNR= -20 dB).

fall into the clutter spectrum ($f_d = 1000$ Hz), the ADT-SFT algorithm can effectively detect the target for both SCNRs (Fig. 8(a) and Fig. 8(b)). There are no false alarms, and the results difference between the two SCNRs is the values of K and H , i.e., $K = 5, H = 82$ for SCNR = -12 dB, and $K = 9, H = 140$ for SCNR = -20 dB. Fig. 9 shows the results of the ADT-SFT algorithm when the target spectrum is completely covered by the clutter spectrum. It can be seen that the detection results of the proposed ADT-SFT are still as good as Fig. 8. But for lower SCNR (Fig. 9(b)), there are a small number of false alarms. The reason is that for Fig. 8, the Doppler SD in clutter background is equivalent to the detection in noise background, while for Fig. 9, the SD is influenced by the clutter background which is stronger than the noise background.

Comparing Fig. 2 to Fig. 5 with Fig. 8 and Fig. 9, we can draw several conclusions: 1) Using the two levels of adaptive detection threshold, the ADT-SFT algorithm can effectively suppress the clutter and improve the moving target detection performance. 2) Due to the influence of strong clutter points in frequency domain, the SCNR after subsampling is seriously deteriorated. 3) To ensure the target's frequency spectrum can go through the threshold, the value of K and H should be bigger, particularly for the lower SCNR. However, this would affect the computational efficiency of the algorithm, which will be discussed in section VI D. In order to deal with the contradiction, we can perform the MTI/AMTI processing on the observed data before ADT-SFT, which can eliminate stronger clutter points near the center of the clutter spectrum, and thereby reduce the influence of the strong clutter points on the first threshold detection result. Then, the algorithm calculation efficiency and detection performance can be balanced. It should be noted that if the target spectrum is too close to the center of the clutter spectrum, it is not appropriate to implement the MTI/AMTI processing before the ADT-SFT algorithm.

B. RESULTS OF MEASURED DATA

The measurement trial was conducted with the Fynmeet dynamic RCS measurement facility at the Over-berg Test Range (OTB). The transmission frequency of radar is 9 GHz, PRF is 5000 Hz, range resolution is 15 m. The cooperated marine target is the WaveRider RIB speedboat with GPS

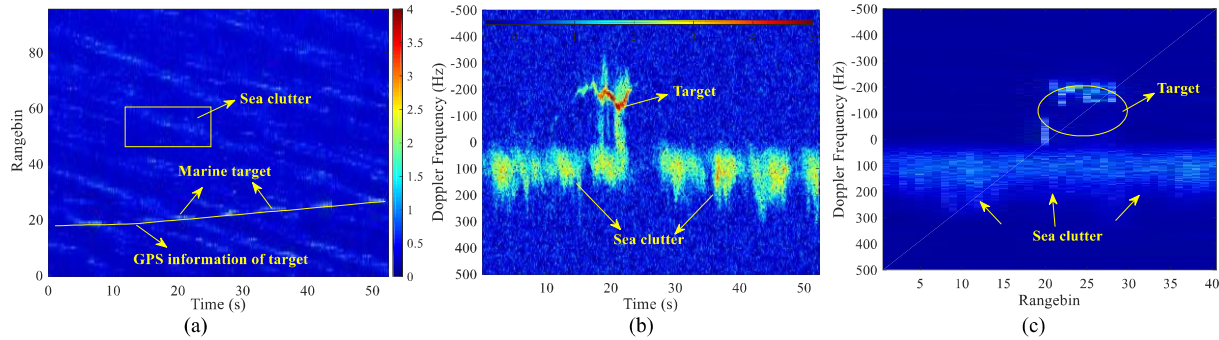


FIGURE 10. Analysis of dataset TFC15_038. (a) Time-range analysis. (b) Time-frequency analysis (22# Rangebin). (c) Range-Doppler analysis.

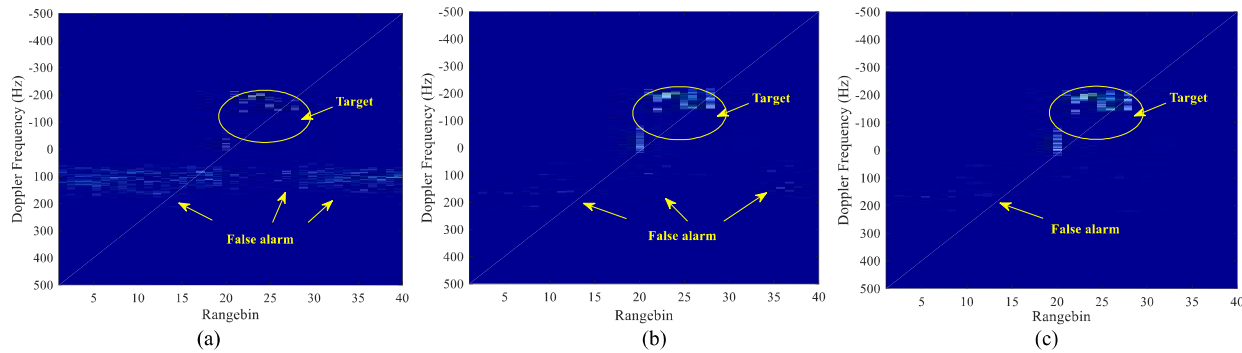


FIGURE 11. Detection results of dataset TFC15_038. (a) Result of SFT. (b) Result of ADT-SFT. (c) Result of AMTI-ADT-SFT.

TABLE 1. Parameters of CSIR datasets.

Data Parameters \ Date	TFC15_038	TFC17_002
Date	2006/08/01	2006/08/03
Observation direction	Upwind	Downwind
Grazing angle (°)	0.445-0.551	0.853-1.27
Observation time (s)	67.793	105
Tracking range (m)	6700.31	3000.94
Wave (m)	3.17	2.77
Douglas scale	4	5

installed. The specifications of Fynmeet radar and the environment parameters can be found in [26] and Table 1.

From the range-time image of TFC15_038 (Fig. 10(a)), it can be seen that the radar observation range covers 96 rangebins. Due to the GPS trajectory labeled in white line, we can easily find the trajectory of real radar returns, which is used for further comparisons. By observing the time-frequency distributions (Doppler spectrum) of each rangebin, e.g. rangebin 22 (Fig. 10(b)), it can be found that the Doppler frequency of the target changes with time, i.e., time-varying, resulting in energy distributed among multiple Doppler bins. Also, during the observation time 52.429 seconds (including $N = 2^{18}$ pulses), the target moves along multiple rangebins, so the target can be considered as a range-Doppler spread target. While the sea clutter spectrum is basically the same for various rangebins, and has the property of spatial stability. In Fig. 10(c), only a small number of target's Doppler points exceed 5 dB above the clutter spectrum.

Then, we compare the detection performances of different algorithms, i.e., SFT (sparsity K is taken as 400), ADT-SFT and AMTI-ADT-SFT. The reason why AMTI is used instead of MTI is because the sea clutter spectrum center of the measured data is not at zero frequency. The related parameters are set as follows: $B = 2048$, $N/B = 128$, $M = 1024$. Fig. 11 shows the detection results of the three methods. There are more clutter false alarms in the range-Doppler detection image of SFT method (Fig. 11(a)), and part of the moving target is lost. This is because that the sparsity K needs to be preset and there is no clutter suppression capability of SFT-based detection method. It can only obtain a small number of strong target Doppler points, and a large number of strong clutter Doppler points are also detected, resulting in false alarms. The false alarms and missing points using the ADT-SFT-based method (Fig. 11(b)) are significantly reduced compared with the SFT algorithm. Using the AMTI processing, ADT-SFT can reduce the influence of strong sea clutter points in the frequency domain (Fig. 11(c)), and therefore the detection performance, i.e., missing points and false alarms, are better than the ADT-SFT algorithm. In order to show the detection performances of the three methods more clearly, Fig. 12 gives the results of the 22# rangebin. The advantage of AMTI-ADT-SFT can be summarized as follows: on the one hand, the AMTI can suppress the strong clutter points in the center of the clutter spectrum and reduce the sparsity in the frequency domain accordingly, so that for the target rangebins (18#~26#), the average value of K passing through the first threshold, is reduced from about 1200 to

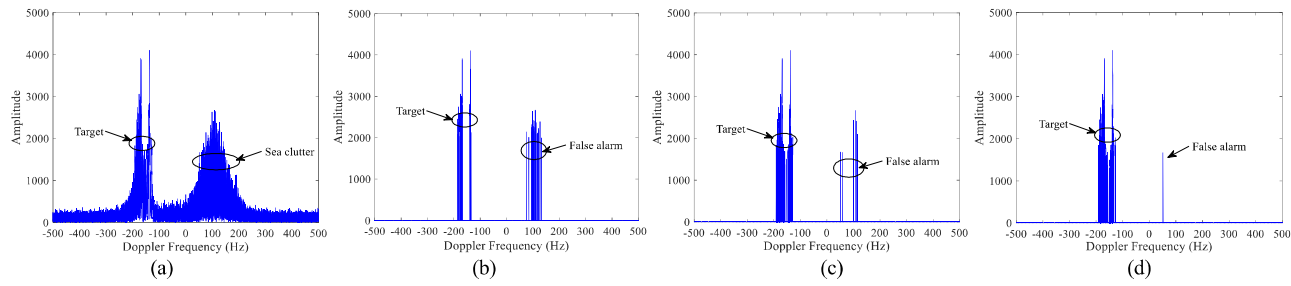


FIGURE 12. Detection results of dataset TFC15_038 (22# Rangebin). (a) FFT. (b) SFT. (c) ADT-SFT. (d) AMTI-ADT-SFT.

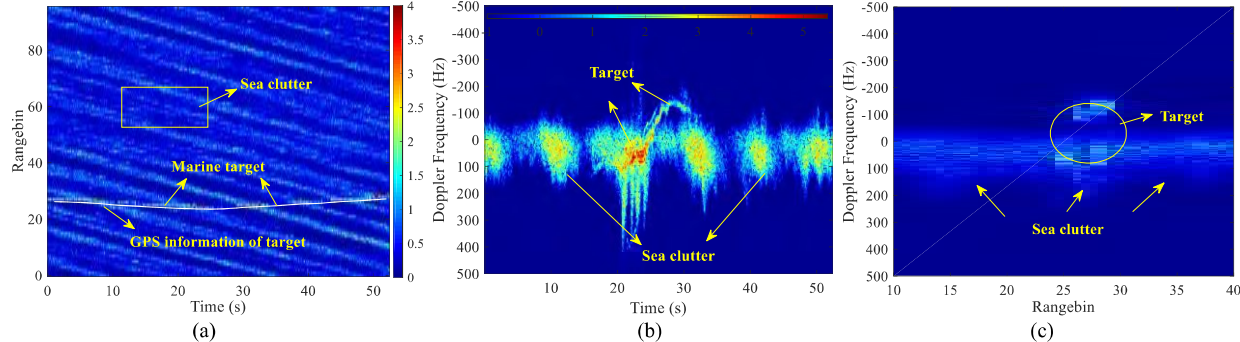


FIGURE 13. Analysis of dataset TFC17_002. (a) Time-range analysis. (b) Time-frequency analysis (25# Rangebin). (c) Range-Doppler analysis.

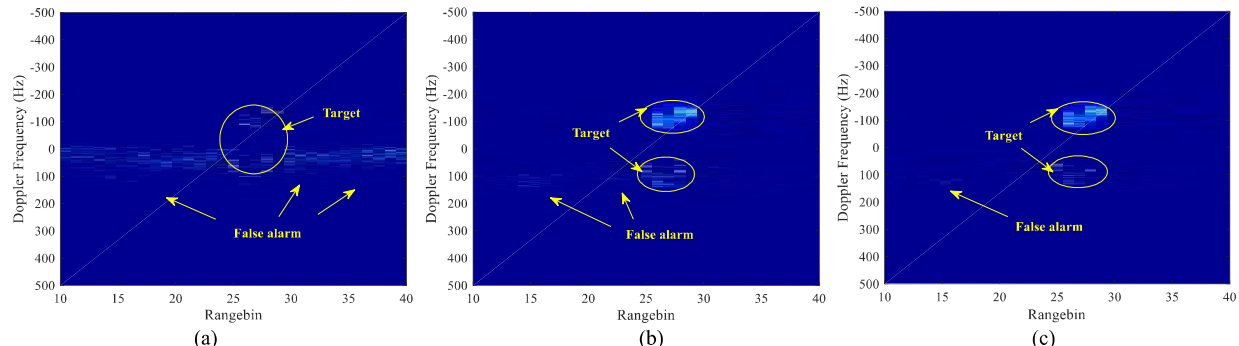


FIGURE 14. Detection results of dataset TFC17_002. (a) Result of SFT. (b) Result of ADT-SFT. (c) Result of AMTI-ADT-SFT.

TABLE 2. Number of false alarms and detected target points.

Number Data	Target points	False alarms
TFC15_038 (22# rangebin)	SFT	97
	SDT-SFT	448
	AMTI-ADT-SFT	451
		303
		6
		1

about 800, which improves the computational efficiency greatly. On the other hand, suppressing strong clutter points can also reduce the SCNR losses caused by flat window filtering, which is also the reason why the missing detection performance is improved in Fig. 11(c) and Fig. 12(d). Table 2 lists the number of false alarms and detected target points in Fig. 12.

Fig 13 to Fig 15 show the data analysis and detection results of the data TFC17_002. The parameters are the same as TFC15_038. Differently, the clutter background of

TFC17_002 is stronger, and most of the target spectrum is covered by the sea clutter spectrum. It can be seen from Fig. 14 and Fig. 15 that when the target spectrum and the clutter spectrum are partially overlapped, the detection results are a little bit worse than that of the previous data TFC15_038. The spectrum points falling into the clutter spectrum are much easier to be lost since the SD corresponding to the partial target Doppler frequencies is carried out in the clutter background. At the same time, compared with Fig. 15(c), the missing points of target in Fig. 15(d) are increased after AMTI processing, which indicates that if the target spectrum is too close to the center of the clutter spectrum, it is not appropriate to implement MTI/AMTI processing before the ADT-SFT algorithm.

C. DETECTION PERFORMANCES ANALYSIS

Assume that the target is moving uniformly, $v = 15 \text{ m/s}$, $\lambda = 0.03 \text{ m}$, $f_d = 1000 \text{ Hz}$, the parameters of clutter are

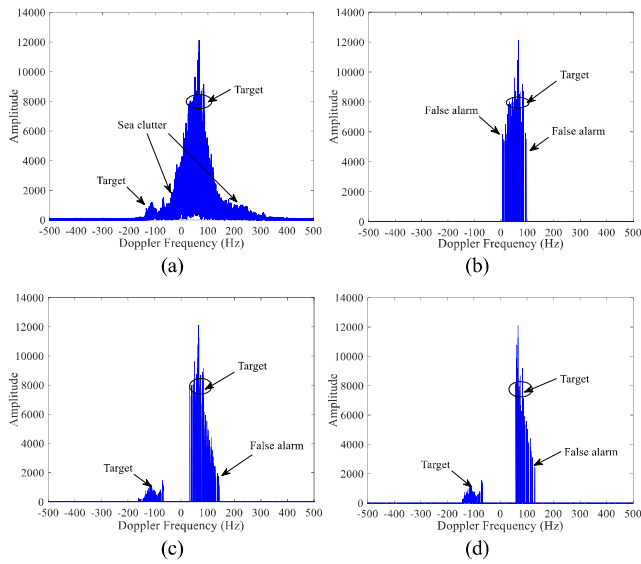


FIGURE 15. Detection results of dataset TFC17_002 (25# Rangebin).
(a) FFT. (b) SFT. (c) ADT-SFT. (d) AMTI-ADT-SFT.

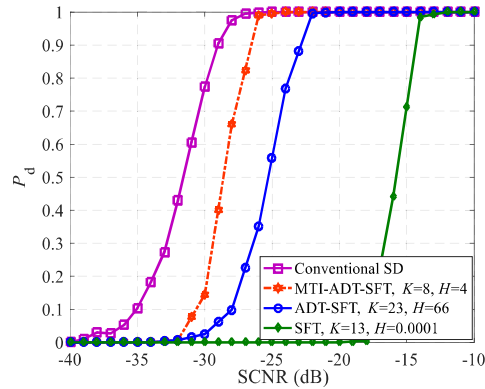


FIGURE 16. Detection performance curve of conventional SD, SFT, ADT-SFT, and MTI-ADT-SFT ($P_{fa} = 10^{-4}$).

the same as section III C, $f_s = 5000$ Hz, $T = 0.0002$ s, $N = 4096$, $B = 256$, $M = 100$. Fig. 16 shows the detection probability P_d versus SCNR curves using the conventional SD, SFT, ADT-SFT, and MTI-ADT-SFT algorithms.

K and H are the average values during the 10^6 Monte Carlo simulations. It can be seen from Fig. 16 that since the conventional SD algorithm constructs the subspace detector by searching all the Doppler channels, it has the best detection performance compared with other three algorithms without considering the computational complexity. The detection performance of the conventional SD, ADT-SFT and MTI-ADT-SFT are obviously higher than SFT by at least 10 dB. It proves that the ADT-SFT algorithm is more suitable for the clutter background than SFT, and can achieve significant improvement in detection performance. Using clutter suppression processing such as MTI and AMTI, the detection performance of the ADT-SFT algorithm can be further improved.

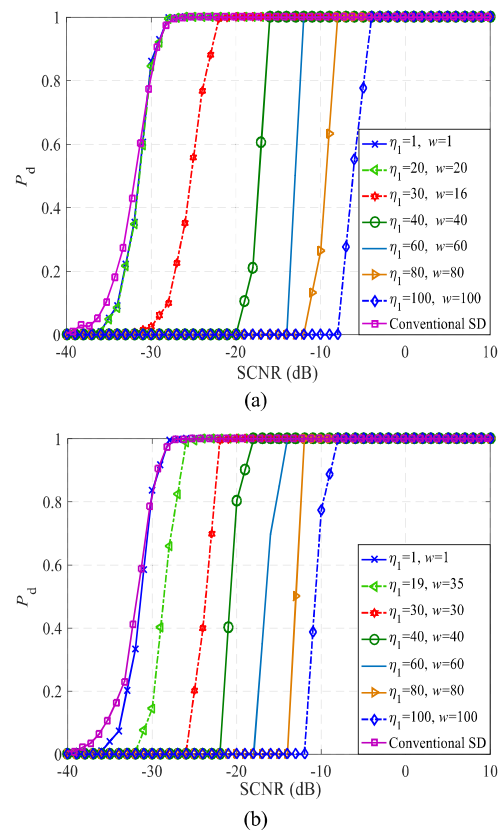


FIGURE 17. Detection performance curves under different η_1 and w .
(a) ADT-SFT. (b) MTI-ADT-SFT.

D. COMPLEXITY ANALYSIS

Compared with the conventional SD algorithm, the ADT-SFT can quickly determine the Doppler frequencies of the suspected target, avoiding search for Doppler frequency one by one, which is computational consuming in case of a large amount of data. Taking the 22# rangebin of TFC15_038 as an example, the number of Doppler channels occupied by the target is about 600. And compared with the total number of Doppler channels, i.e., 2^{18} , the target's Doppler channel only occupies 0.23%, which obviously indicates that ADT-SFT can significantly reduce the computational complexity compared to conventional SD algorithm.

Specifically, the computational complexity of the ADT-SFT algorithm is mainly affected by the K and H value, and the H value determines the searching times of the subspace detector. Therefore, when the subspace detector is complex, the H value counts for more. The K and H values are directly controlled by the first threshold η_1 and the Occurrence Value w , and the bigger of η_1 and w , the smaller the K and H . Fig. 17 shows the P_d curves of the ADT-SFT and the MTI-ADT-SFT with different η_1 and w . We can see that η_1 and w have a significant impact on the detection performance. The lower η_1 and w , the bigger K and H , and the detection performance is much closer to the conventional SD algorithm, but the higher the computational complexity.

TABLE 3. List of H under different η_1 and w .

η_1	1	19	20	30	30	40	60	100
w	1	35	20	16	30	40	60	100
H^1	4096	148	120	66	24.7	2.1	0	0
H^2	4096	4	2	1	0	0	0	0

H^1 : ADT-SFT;

H^2 : MTI-ADT-SFT

Table 3 gives the relations of η_1 , w , and H quantitatively in the case without the target. H can reflect the computational burden from another point of view, i.e., the searching times for the Doppler frequencies. We can conclude from Fig. 17 and Table 3: 1) MTI processing can effectively reduce the number of false alarms of the ADT-SFT algorithm, thereby improving computational efficiency. 2) The lower η_1 and w , the closer the detection performance to the conventional SD, but at the same time resulting in a bigger H , which will increase the computation burden. Therefore, we should choose the proper η_1 and w in order to find the balance between computational complexity and the detection performance. In addition, it should be noted that the proposed algorithm has more remarkable advantages in terms of operational efficiency when the signal size is larger. Moreover, the ADT-SFT algorithm is more suitable for stationary signals, and the detection performance will be degraded for maneuvering targets with complex motions.

VII. CONCLUSIONS

In this paper, based on the detail analysis of SFT and RSFT, which are not applicable to moving target detection in clutter background, a novel algorithm named as ADT-SFT is proposed. The simulations and experiments using real radar data in complex sea clutter verified the advantages:

1) ADT-SFT algorithm does not require knowledge of the exact sparsity K , and is more suitable for clutter background than SFT and RSFT, which is more practicable.

2) ADT-SFT algorithm only needs to construct a subspace detector for a small number of suspected target frequencies points, which can reduce the computational complexity greatly compared with the conventional SD algorithm.

3) For lower SCNR, the performance of ADT-SFT when the target spectrum does not fall into the clutter spectrum is superior to the case when the target spectrum is covered by the clutter spectrum.

4) MTI/AMTI can eliminate the strong clutter points in frequency domain and thus can be used for clutter suppression, which would further improve the detection performance of the ADT-SFT algorithm. However, the use of MTI/AMTI should be careful especially for the slowly moving target.

5) The K and H of the ADT-SFT have a great influence on the performance, and they are directly influenced by η_1 and w . It needs to be balanced between computational complexity and detection performance.

In a word, the ADT-SFT-based moving target detection method not only takes the advantage of the SFT in terms of

computational efficiency, but also uses the subspace detector for good detection performance, which provides an effective way to improve the radar target detection performance with limited radar resources and complex clutter environment. In the future, we will further verify the moving target detection performance of the proposed algorithm in different clutter environments.

ACKNOWLEDGMENT

The authors would like to thank the anonymous reviewers for the valuable comments and suggestions.

REFERENCES

- [1] X. Chen, Y. Huang, N. Liu, J. Guan, and Y. He, "Radon-fractional ambiguity function-based detection method of low-observable maneuvering target," *IEEE Trans. Aerosp. Electron. Syst.*, vol. 51, no. 2, pp. 815–833, Apr. 2015.
- [2] X. Chen, J. Guan, N. Liu, W. Zhou, and Y. He, "Detection of a low observable sea-surface target with micromotion via the radon-linear canonical transform," *IEEE Geosci. Remote Sens. Lett.*, vol. 11, no. 7, pp. 1225–1229, Jul. 2014.
- [3] X. Chen, J. Guan, X. Yu, and Y. He, "Radar detection for moving target in short-time sparse fractional Fourier transform domain," *Acta Electron. Sinica*, vol. 45, no. 12, pp. 3030–3036, 2017.
- [4] Z. Zhang, Y. Xu, J. Yang, X. Li, and D. Zhang, "A survey of sparse representation: Algorithms and applications," *IEEE Access*, vol. 3, no. 1, pp. 490–530, May 2015.
- [5] S. Liu et al., "Sparse discrete fractional Fourier transform and its applications," *IEEE Trans. Signal Process.*, vol. 62, no. 24, pp. 6582–6595, Dec. 2014.
- [6] X. L. Chen, J. Guan, Y. L. Dong, and Z. J. Zhao, "Sea clutter suppression and micromotion target detection in sparse Domain," *Acta Electronica Sinica*, vol. 44, no. 4, pp. 860–867, 2016.
- [7] F. Milioz and M. Davies, "Sparse detection in the chirplet transform: Application to FMCW radar signals," *IEEE Trans. Signal Process.*, vol. 60, no. 6, pp. 2800–2813, Jun. 2012.
- [8] X. Chen, X. Yu, J. Guan, and Y. He, "An effective and efficient long-time coherent integration method for highly maneuvering radar target in sparse domain," in *Proc. 4th Int. Workshop Compressed Sens. Theory Appl. Radar Sonar Remote Sens. (CoSeRa)*, Sep. 2016, pp. 124–127.
- [9] J. Liu, X. Li, X. Gao, and Z. Zhuang, "High-speed target isar imaging via compressed sending based on sparsity in fractional Fourier domain," *Chin. J. Electron.*, vol. 22, no. 3, pp. 648–654, 2013.
- [10] Y. Tang, Y. Zhang, and Z. Guo, "Approach to weak signal extraction and detection via sparse representation," *J. Commun.*, vol. 36, no. s1, pp. 215–223, 2015.
- [11] H. Hassanieh, P. Indyk, D. Katabi, and E. Price, "Simple and practical algorithm for sparse Fourier transform," in *Proc. 23rd Annu. ACM-SIAM Symp. Discrete Algorithms*, Kyoto, Japan, Jan. 2012, pp. 1183–1194.
- [12] H. Hassanieh, P. Indyk, D. Katabi, and E. Price, "Nearly optimal sparse Fourier transform," in *Proc. 44th Annu. ACM Symp. Theory Comput.*, New York, USA, May 2012, pp. 563–578.
- [13] J. Schumacher, "High performance sparse fast Fourier transform," M.S. thesis, Dept. Comput. Sci., ETH Zurich, Zurich, Switzerland, 2013.
- [14] A. C. Gilbert, P. Indyk, M. Iwen, and L. Schmidt, "Recent developments in the sparse Fourier transform: A compressed Fourier transform for big data," *IEEE Signal Process. Mag.*, vol. 31, no. 5, pp. 91–100, Sep. 2014.
- [15] X. Chen, J. Guan, Y. He, and X. Yu, "High-resolution sparse representation and its applications in radar moving target detection," *J. Radars*, vol. 6, no. 3, pp. 239–251, 2017.
- [16] C. Pang, S. Liu, and Y. Han, "High-speed target detection algorithm based on sparse Fourier transform," *IEEE Access*, vol. 6, pp. 37828–37836, 2018.
- [17] S. Wang, V. M. Patel, and A. Petropulu, "RSFT: A realistic high dimensional sparse Fourier transform and its application in radar signal processing," in *Proc. IEEE Mil. Commun. Conf.*, Nov. 2016, pp. 888–893.
- [18] A. Rauh and G. R. Arce, "Optimized spectrum permutation for the multidimensional sparse FFT," *IEEE Trans. Signal Process.*, vol. 65, no. 1, pp. 162–172, Jan. 2017.

- [19] G.-L. Chen, S.-H. Tsai, and K.-J. Yang, "On performance of sparse fast Fourier transform and enhancement algorithm," *IEEE Trans. Signal Process.*, vol. 65, no. 21, pp. 5716–5729, Nov. 2017.
- [20] S. Wang, V. M. Patel, and A. Petropulu, "The robust sparse Fourier transform (RSFT) and its application in radar signal processing," *IEEE Trans. Aerosp. Electron. Syst.*, vol. 53, no. 6, pp. 2735–2755, Dec. 2017.
- [21] H. Rohling, "Radar CFAR thresholding in clutter and multiple target situations," *IEEE Trans. Aerosp. Electron. Syst.*, vol. 19, no. 4, pp. 608–621, Jul. 1983.
- [22] M. E. Smith and P. K. Varshney, "Intelligent CFAR processor based on data variability," *IEEE Trans. Aerosp. Electron. Syst.*, vol. 36, no. 3, pp. 837–847, Jul. 2000.
- [23] J. S. Goldstein, I. S. Reed, and P. A. Zulch, "Multistage partially adaptive STAP CFAR detection algorithm," *IEEE Trans. Aerosp. Electron. Syst.*, vol. 35, no. 2, pp. 645–661, Apr. 1999.
- [24] S. Zhong, X. Wang, W. Wang, and J. Liu, "Recent advances in the sparse Fourier transform," *Trans. Beijing Inst. Technol.*, vol. 37, no. 2, pp. 111–118, 2017.
- [25] W. Liu, T. Jian, H. Yang, S. Li, H. Wang, and Y. Wang, "Tunable multi-channel adaptive detector for mismatched subspace signals," *J. Electron. Inf. Technol.*, vol. 38, no. 12, pp. 3011–3017, 2016.
- [26] H. J. de Wind, J. E. Cilliers, and P. L. Herselman, "DataWare: Sea clutter and small boat radar reflectivity databases [Best of the Web]," *IEEE Signal Process. Mag.*, vol. 27, no. 2, pp. 145–148, Mar. 2010.



XIAOHAN YU was born in Hebei, China, in 1991. She received the M.S. degree in information and communication engineering from Naval Aviation University (NAU), Yantai, China, in 2015, where she is currently pursuing the Ph.D. degree in information and communication engineering.

Her main research interests include radar moving target detection and sparse signal processing.



XIAOLONG CHEN (M'12) was born in Yantai, Shandong, China, in 1985. He received the bachelor's and master's degrees in signal and information processing and the Ph.D. degree in radar signal processing from Naval Aviation University (NAU), in 2010 and 2014, respectively.

From 2015 to 2017, he was a Lecturer with the Marine Target Detection Research Group, NAU, where he lectures radar principle, and is currently an Associate Professor. He has published more than 70 academic articles and two books and holds 23 national invention patents. He has given more than 20 speeches on radar signal processing, especially marine target. His current research interests include marine target detection, micro-Doppler, and sea clutter suppression.

Dr. Chen has been a member of the 2015 and 2018 IET International Radar Conference Technical Committees. He was selected as the Young Talents Program of the China Association for Science and Technology, in 2016, and received the Excellent Doctor Dissertation of CIE. In 2017, he received the Chinese Patent Award. He received four excellent papers in the 2016 International Radar Conference, the 2017 EAI International Conference on Machine Learning and Intelligent Communications (MLICOM 2017), the 14th National Radar Conference, and the 2019 IEEE 2nd International Conference on Electronic Information and Communication Technology (ICEICT 2019), respectively. He was the Section Chair of the 2016 International Conference on Mathematical Characterization, Analysis and Applications of Complex Information, the 2017 MLICOM, 2017 International Conference on Radar Systems (U.K.), and 2019 ICEICT. He was selected for a URSI Young Scientist Award in the 2019 URSI Asia-Pacific Radio Science Conference. He is an Associate Editor of the IEEE ACCESS and frequently a reviewer for the IEEE SPL, IEEE TGRS, IEEE GRSL, IEEE JSTARS, IET RSN, IET SP, IET EL, DSP, and many international conferences.



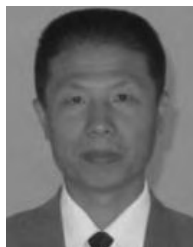
YONG HUANG was born in Hunan, China, in 1979. He received the M.S. and Ph.D. degrees in information and communication engineering from Naval Aviation University (NAU), in 2005 and 2010, respectively.

From 2011 to 2016, he was a Lecturer with the Department of Electronic and Information Engineering, NAU, where he is currently an Associate Professor. His current research interests include radar signal processing and clutter rejection.



LIN ZHANG was born in Shandong, China, in 1986. He received the M.S. and Ph.D. degrees in information and communication engineering from Naval Aviation University (NAU), in 2011 and 2016, respectively.

He is currently a Lecturer with the Department of Electronic and Information Engineering, NAU. His current research interest includes signal detection and estimation.



JIAN GUAN (M'07) received the Ph.D. degree in electronic engineering from Tsinghua University, Beijing, China, in 2000.

He is currently a Professor with Naval Aviation University (NAU). His research interests include radar target detection and tracking, image processing, and information fusion. He has authored numerous papers in his areas of expertise and holds 21 national invention patents. He has authored two books related to radar detection.

Dr. Guan is a Senior Member of the CIE and a Committee Member of the Radio Positioning Technology Branch, CIE. He received the National Excellent Doctoral Dissertation Prize and the Realistic Outstanding Youth Practical Engineering Award of CAST and was selected for National Talents Engineering of Ministry of Personnel of China. He has served in the technical committee of many international conferences on radar. He is on the Editorial Boards of many radar related journals.



YOU HE was born in Jilin, China, in 1956. He received the Ph.D. degree in electronic engineering from Tsinghua University, Beijing, China, in 1997.

He is currently a Professor with Naval Aviation University (NAU). He has published over 300 academic articles. He has authored *Radar Target Detection and CFAR Processing* (Tsinghua University Press), *Multisensor Information Fusion With Applications*, and *Radar Data Processing With Applications* (Publishing House of Electronics Industry). His current research interests include detection and estimation theory, CFAR processing, distributed detection theory, and multisensor information fusion.

Dr. He is a Fellow Member of the Chinese Institute of Electronics. He has been a member of the Chinese Academy of Engineering, since 2013. In 2017, he received the top prize in science and technology of Shandong Province. He currently serves on the Editorial Boards of the *Journal of Data Acquisition and Processing*, *Modern Radar*, *Fire Control & Command Control*, and *Radar Science and Technology*.